AFRL-RZ-WP-TP-2012-0103

IN SITU CREATION OF NANOPARTICLES FROM YBCO BY PULSED LASER DEPOSITION (POSTPRINT)

Paul N. Barnes and Timothy J. Haugan

Mechanical Energy Conversion Branch
Energy/Power/Thermal Division

P. Terry Murray

University of Dayton

Richard Rogow and Glen P. Perram

Air Force Institute of Technology

FEBRUARY 2012

AIR FORCE RESEARCH LABORATORY
PROPULSION DIRECTORATE
WRIGHT-PATTERSON AIR FORCE BASE, OH 45433-7251
AIR FORCE MATERIEL COMMAND
UNITED STATES AIR FORCE

REPORT DOCUMENTATION PAGE

Form Approved
OMB No. 0704-0188

1. REPORT DATE *(DD-MM-YY)*	2. REPORT TYPE	3. DATES COVERED *(From - To)*
February 2012	Journal Article Postprint	01 September 2000 – 01 September 2002

4. TITLE AND SUBTITLE

IN SITU CREATION OF NANOPARTICLES FROM YBCO BY PULSED LASER DEPOSITION (POSTPRINT)

5a. CONTRACT NUMBER
In-house

5b. GRANT NUMBER

5c. PROGRAM ELEMENT NUMBER
62203F

6. AUTHOR(S)

Paul N. Barnes and Timothy J. Haugan (AFRL/RZPG)
P. Terry Murray (University of Dayton)
Richard Rogow and Glen P. Perram (Air Force Institute of Technology)

5d. PROJECT NUMBER
3145

5e. TASK NUMBER
32

5f. WORK UNIT NUMBER
314532Z9

7. PERFORMING ORGANIZATION NAME(S) AND ADDRESS(ES)

Mechanical Energy Conversion Branch (AFRL/RZPG)
Energy/Power/Thermal Division
Air Force Research Laboratory, Propulsion Directorate
Wright-Patterson Air Force Base, OH 45433-7251
Air Force Materiel Command, United States Air Force

University of Dayton
Dayton, OH

Air Force Institute of Technology
Wright-Patterson AFB, OH 45433

8. PERFORMING ORGANIZATION REPORT NUMBER
AFRL-RZ-WP-TP-2012-0103

9. SPONSORING/MONITORING AGENCY NAME(S) AND ADDRESS(ES)

Air Force Research Laboratory
Propulsion Directorate
Wright-Patterson Air Force Base, OH 45433-7251
Air Force Materiel Command
United States Air Force

10. SPONSORING/MONITORING AGENCY ACRONYM(S)
AFRL/RZPG

11. SPONSORING/MONITORING AGENCY REPORT NUMBER(S)
AFRL-RZ-WP-TP-2012-0103

12. DISTRIBUTION/AVAILABILITY STATEMENT

Approved for public release; distribution unlimited.

13. SUPPLEMENTARY NOTES

Journal article published in *Physica C*, Vol. 377, 2002. Work on this effort was completed in 2002.

PA Case Number: ASC-01-1693; Clearance Date: 19 Nov 2002.

14. ABSTRACT

Nanoparticles created by the laser ablation of YBCO are reported. The experimental procedure entailed pulsed laser deposition (PLD) of YBCO at a high background pressure of 5 Torr O_2. The sizes of the nanoparticles range from ~3 to 5 nm and are typical of the depositions made using laser energies of 50 mJ per pulse. Optical emission spectroscopy was used to characterize the PLD plume. Under nanoparticle deposition conditions, the visible plume emission is very weak. Even so, the distribution among electronically excited states cannot be described by a single temperature. The plume remains collisionally dynamic even at high pressures and low laser energies and retains considerable excitation when nanoparticles are formed.

15. SUBJECT TERMS

high-temperature superconductors, aerosol nanoparticle formation, pulsed laser deposition, optical emission spectroscopy of PLD plumes, $YBa_2Cu_3O_{7-\delta}$

16. SECURITY CLASSIFICATION OF:			17. LIMITATION OF ABSTRACT:	18. NUMBER OF PAGES	19a. NAME OF RESPONSIBLE PERSON (Monitor)
a. REPORT	b. ABSTRACT	c. THIS PAGE			Timothy J. Haugan
Unclassified	Unclassified	Unclassified	SAR	14	19b. TELEPHONE NUMBER *(Include Area Code)* N/A

ELSEVIER

Physica C 377 (2002) 578–584

PHYSICA C

www.elsevier.com/locate/physc

In situ creation of nanoparticles from YBCO by pulsed laser deposition

Paul N. Barnes [a,*], P. Terry Murray [b], Tim Haugan [a], Richard Rogow [c], Glen P. Perram [c]

[a] *Air Force Research Laboratory/PRPG, Building 450, 2645 Fifth street, Ste. 13, Wright-Patterson AFB, OH 45433-7919, USA*
[b] *University of Dayton, Dayton, OH 45419, USA*
[c] *Air Force Institute of Technology, Wright-Patterson AFB, OH 45433, USA*

Received 6 September 2001; received in revised form 8 January 2002; accepted 11 January 2002

Abstract

Nanoparticles created by the laser ablation of YBCO are reported. The experimental procedure entailed pulsed laser deposition (PLD) of YBCO at a high background pressure of 5 Torr O_2. The sizes of the nanoparticles range from ~3 to 5 nm and are typical of the depositions made using laser energies of 50 mJ per pulse. Optical emission spectroscopy was used to characterize the PLD plume. Under nanoparticle deposition conditions, the visible plume emission is very weak. Even so, the distribution among electronically excited states cannot be described by a single temperature. The plume remains collisionally dynamic even at high pressures and low laser energies and retains considerable excitation when nanoparticles are formed.

PACS: 74.72.B; 74.60.G; 81.05.Y
Keywords: $YBa_2Cu_3O_{7-\delta}$; Nanoparticles

1. Introduction

The high temperature superconducting (HTS) $YBa_2Cu_3O_{7-x}$ (YBCO) coated conductor has demonstrated the ability for excellent performance at liquid nitrogen temperature maintaining current densities above 10^5 A/cm^2 even at a few tesla [1]. Even so, improvements can still be made in its overall properties as well as in producing longer lengths of the conductor [2]. Achieving these improvements will allow availability of the YBCO coated conductor for a variety of applications. Some of the commercial applications of the YBCO conductor include power transmission cables, fault current limiters, transformers, generators and motors. The military is actively pursuing HTS motor and generator development programs that will eventually incorporate the YBCO coated conductor as it becomes available [3].

A variety of methods are used to deposit the YBCO such as chemical solution, MOCVD, combustion chemical vapor deposition, and pulsed laser deposition (PLD) [4–9]. Even though many

* Corresponding author. Tel.: +1-937-255-4410; fax: +1-937-656-4095.
E-mail address: paul.barnes@wpafb.af.mil (P.N. Barnes).

0921-4534/02/$ - see front matter © 2002 Published by Elsevier Science B.V.
PII: S0921-4534(02)00919-X

of the methods have demonstrated the ability to deposit YBCO with $>10^6$ A/cm^2, 77 K, self-field on small samples, PLD is still largely used for depositing high quality YBCO films because of the technique's past capability to readily create these high quality samples. However, PLD is usually considered a more expensive method for production of long lengths of coated conductor and hence the pursuit of other methods of fabrication. Even so, Los Alamos National Laboratory has demonstrated higher rates of deposition by PLD using an industrial laser [10].

The high temperature superconductors, type II superconductors, at typical operating temperatures do not exhibit the full Meissner effect but allows the penetration of quantized magnetic flux tubes or vortices through the material. As such, the effectiveness of the superconductor is decreased, for example, as lower in-field critical current densities. Such losses can be minimized by the addition of defect sites within the film that will help pin the magnetic vortices to the defect [2]. Methods for generating different types of defects for flux pinning as well as the associated effects is still a subject of investigation [8,11–15].

One possible type of defect that might be useful for flux pinning in YBCO is nanoparticles of alternate material dispersed throughout the superconductor. Nanoparticles are extremely small pieces of matter that have dimensions on the order of a few nm. It may well be possible to use nanoparticles of YBCO itself as the defect sites for flux pinning. YBCO must be appropriately textured or oriented since the supercurrents flow through the planes perpendicular to the *c*-axis of the material and the YBCO nanoparticles may not be properly aligned or even phased. Even so, subsequent growth of oriented YBCO may well be affected by the presence of the nanoparticles, but this is presently not known. For the purposes of flux pinning all that is needed are for the nanoparticles of YBCO to act as defect sites. The advantage of using YBCO for the nanoparticles as opposed to some other material is compatibility and no additional target.

In recent years, there has been considerable interest in elucidating the mechanism(s) responsible for the strong photoluminescence arising from nanometer-sized structures in porous Si [16–18]. This prompted several studies in which nanoparticles of Si were generated by pulsed laser ablation [19–29]. These studies demonstrated that such particles can indeed be generated in this way and that the nanoparticle size distribution is determined by a number of factors including target–substrate distance, repetition rate, and the atomic weight of the background gas.

The nanoparticles of Si were generated by carrying out the laser ablation of Si at fairly high pressures (on the order of several Torr) [30,31]. Presumably, the mechanism for nanoparticle generation involves ablation of primarily atomic species, and the nucleation of these atoms into nanometer-sized particles by virtue of the high background pressure. This identical procedure was adopted to synthesize nanoparticles from YBCO in situ. This paper reports on the feasibility of synthesizing YBCO nanoparticles.

2. Experimental

The experimental procedure entailed irradiating a YBCO target of bulk material in a typical PLD chamber used for making thin film YBCO with the output of a KrF ($\lambda = 248$ nm) excimer laser at a high background pressure of 5 Torr O_2. O_2 was used since this gas is used for deposition of thin film YBCO. The laser was operated at a 4 Hz repetition rate with an energy between 40 and 200 mJ per pulse. The target to substrate distance was 25 mm with a deposition time of 2 min. The heater assembly was replaced with an assembly to catch the nanoparticles that consisted of a single crystal Si substrate. As such the substrate was not heated. A number of experiments were carried out that entailed ablating the same YBCO target used previously. The particles thus synthesized were analyzed by transmission electron microscopy (TEM), by atomic force microscopy (AFM) and by scanning tunneling microscopy (STM). A holey carbon substrate was used to collect the particles for the TEM analysis.

Optical emission spectroscopy was also used to characterize the PLD plume under nanoparticle deposition conditions. An Acton 0.25 m

monochromator and Princeton Instruments 1024 element diode array, or Optical Multichannel Analyzer (OMA), with a fiber bundle coupled to a 3.5 cm diameter, 3.0 cm focal length lens was used to resolve the visible emission from the plume. The instrumental resolution was 0.4 nm with a 68 nm bandwidth. As many as 34 spectral segments were acquired to span the wavelength range 0.25–1.0 μm. The OMA was employed in a non-gated mode, providing a time averaged spectra for 80 laser pulses. The system was calibrated for relative spectral response using an 800 K blackbody source. In addition, a Canon XL-1 digital video camera was used to record time integrated plume imagery.

3. Results and discussion

Shown in Fig. 1a and b are AFM micrographs of the deposited YBCO material produced by 50 and 100 mJ laser pulses, respectively. This micrograph in Fig. 1a was obtained from a substrate that was placed 25 mm from the target. The spherical shapes seen in this micrograph confirm that nanoparticles of YBCO were synthesized by laser ablation. The sizes of the particles in this micrograph range from ~3 to 5 nm and are typical of the depositions made. The micrograph shown in Fig. 1b is representative of the depositions obtained by using laser energies of 100 mJ per pulse or higher. No nanoparticles are seen at the higher laser energies and the substrate is covered by a continuous amorphous film. These results are consistent with the TEM results—higher laser energy produces no nanoparticles.

3.1. Nanoparticle formation

Fig. 2a displays a TEM micrograph representative of the nanoparticles grown using a laser energy of 50 mJ per pulse. This figure was obtained in the dark field mode, meaning that light areas in the figure represent regions of the deposit that were crystalline. Examination of this micrograph under higher magnification indicates that these particles are on the order of 5 nm and indicates that nanoparticles were synthesized from the YBCO. Shown in Fig. 2b is the electron diffraction pattern obtained from the same sample. The presence of rings in the pattern confirms that the material is indeed crystalline; however, the width of the rings (the fuzziness) indicates the crystallites to be very small with dimensions on the order of a few nm.

The interaction of nanosecond laser radiation with the target results primarily in the ejection of neutral and singly ionized atomic Ba, Y and Cu. If this is done in a high vacuum, the ejected atoms leave the target with hyperthermal energies (on the order of several eV's) and continue their rectilinear trajectories until they strike an appropriate substrate. Thereby, a thin film of the target material is formed on the substrate. This is the basis for conventional PLD. If, on the other hand, the laser/

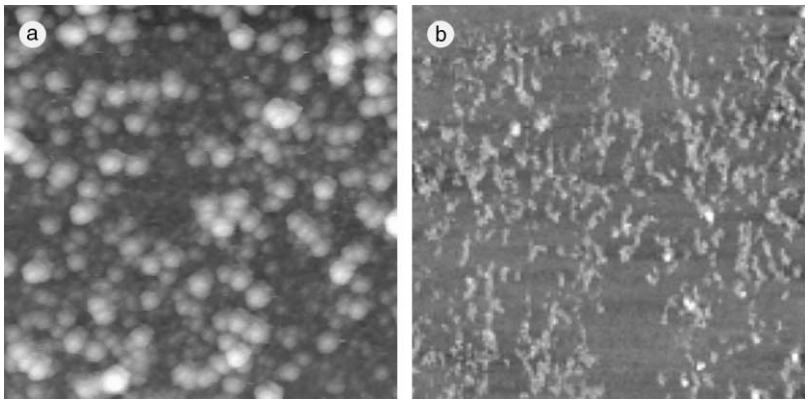

Fig. 1. AFM micrographs of: (a) YBCO nanoparticles and (b) amorphous YBCO.

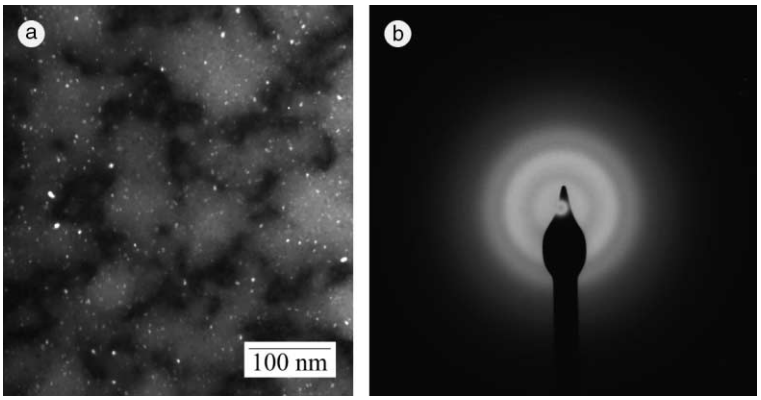

Fig. 2. YBCO nanoparticles: (a) TEM micrograph (dark field mode) of nanoparticles grown using a laser energy of 50 mJ per pulse and (b) electron diffraction pattern obtained from same sample.

material interaction occurs at a high pressure (a few Torr), the ejected species are more quickly thermalized by the ambient gas. This allows them sufficient time to nucleate in the gas phase to form molecules and larger conglomerations. If the residence time of these species in the gas phase is sufficiently long, the background pressure is high enough, these particles can agglomerate to make nanoparticles of the target material.

However, from the results presented, the formation of the nanoparticles is clearly not only a function of the higher pressure but also of the laser energy. There are several possible explanations. One possibility is that the plasma generated by the higher energy laser pulse is too energetic to allow nanoparticles to be thermalized and agglomerate within the 25 mm nucleation zone. Another possibility is that the nanoparticles were indeed formed under the 100 mJ conditions but were subsequently destroyed by exposure to the (higher energy) flux of ablated material at 100 mJ, or the nanoparticles themselves have sufficient kinetic energy to dissociate upon impact with the substrate.

3.2. Optical diagnostics

Nanoparticle formation is observed only when the visible plume emission is nearly totally extinguished. At the 5 Torr oxygen pressure, the visible plume extends only about 7 mm from the target. In contrast, for oxygen pressures of about 200 mTorr, typical of YBCO superconducting film production, the plume fills the 25 mm distance to the substrate. The high pressure plumes are considerably less stable and an interesting Y-shaped structure is often observed. One leg of the Y-shape is directed normal to the target surface. The second leg of the plume is directed along the incident laser beam.

The visible emission spectra from the high pressure plumes were recorded in the wavelength range 0.25–1.0 μm at about 0.4 nm resolution for laser energies of 40–200 mJ. A small segment of the spectrum near 650 nm for a laser energy of 200 mJ/pulse is shown in Fig. 3. Atomic emission lines from neutral and singly ionized Ba, Y, and Cu, as well as molecular emission from YO, are readily identified throughout the spectra. The spectrum of Fig. 3 was chosen to illustrate the seven fine structure lines from the neutral barium, Ba I ($5d6p\ ^3D^o_J \rightarrow 6s5d\ ^3D_J$) transitions. The intensity has been calibrated to correct for relative spectral response. A least squares fit of the data to a series of Lorentzian broadened lines is also shown and was used to determine the relative intensities of the various spectral features. The relative intensities are linearly proportional to the number density of the emitting states:

$$\frac{I_i}{I_j} = \left(\frac{A_{ik}}{A_{jl}}\right)\frac{N_i}{N_j} \tag{1}$$

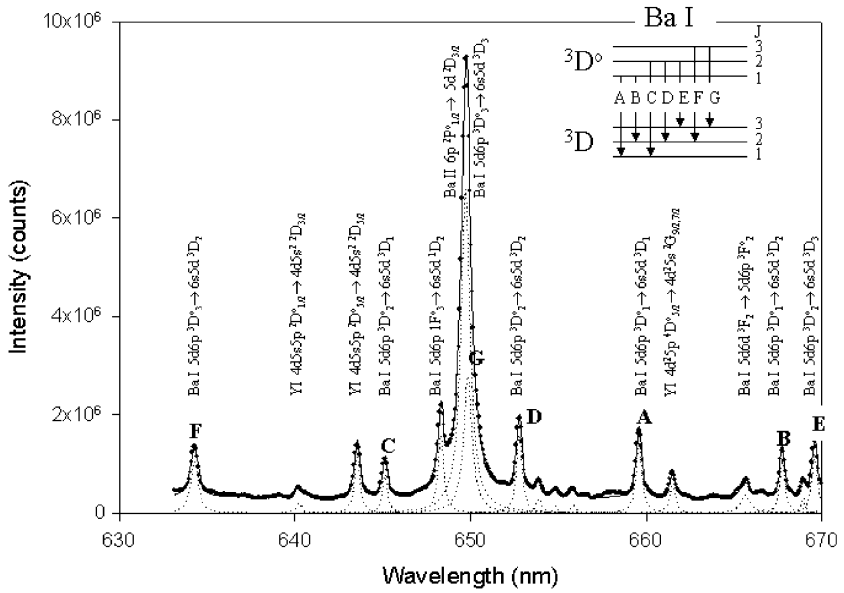

Fig. 3. Portion of the visible plume emission spectrum showing the seven components of the Ba I 5d6p ^{3}D° → 6s5d ^{3}D fine structure. The spectrum was fit to a series of Lorentzian profiles (···) to determine the relative intensities of the various spectral features.

where I_i = intensity of emission from state i, A_{ik} = spontaneous emission rate from state i to state k, and N_i = number density in the emitting state i.

The intensities of isolated spectral features were determined to less than 5% for all but the weakest lines. For blended lines, such as the feature near $\lambda = 649.7$ nm involving both Ba I and Ba II lines, the fraction of the intensity attributed to each feature is poorly determined, with errors exceeding 50%. The spontaneous emission rates, A_{ik}, were obtained from a recent compilation [32].

Fig. 4 shows the visible emission from neutral Ba (■) $^1P_1 \rightarrow {}^1S_0$ at $\lambda = 553.5$ nm, Y (◆) $^2D^o_{5/2} \rightarrow {}^2D_{5/2}$ at $\lambda = 643.5$ nm, and Cu (o) $^2P^o_{3/2} \rightarrow {}^2D_{5/2}$ at $\lambda = 510.6$ nm, as a function of laser energy. Note that there exists a common laser energy threshold for significant emission near 40 mJ. The visible plume emission is very weak under conditions for YBCO nanoparticle formation. Apparently the plume must be depleted of most of its energy before the formation of nanoparticles can be supported. Both gas phase clustering and the survival of deposited YBCO nanoparticles would be aided by a less energized PLD plume. The relative intensity of the three atomic species is determined by the electronic state distribution and does not reflect the total atomic content in the plume. The approximately linear dependence on laser energy suggests the emission intensity depends primarily on the total number of ablated atoms.

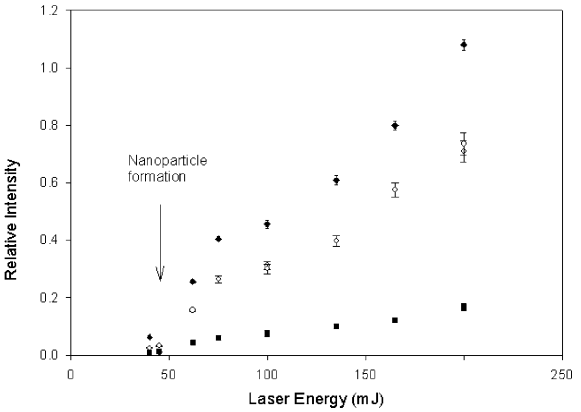

Fig. 4. Emission intensity from neutral Ba (■) $^1P_1 \rightarrow {}^1S_0$ at $\lambda = 553.5$ nm, Y (◆) $^2D^o_{5/2} \rightarrow {}^2D_{5/2}$ at $\lambda = 643.5$ nm, and Cu (○) $^2P^o_{3/2} \rightarrow {}^2D_{5/2}$ at $\lambda = 510.6$ nm, as a function of laser energy.

The plume retains high electronic temperatures and significant ionization, even at the lower laser energies associated with nanoparticle formation. The distribution of electronically excited state populations can be determined from the emission spectra [33]. The relative amplitudes of the various lines can be used to extract an electronic temperature using a Boltzmann distribution:

$$\frac{N_i}{N_j} = \frac{g_i}{g_j} e^{-\Delta E_{i,j}/k_B T} \quad (2)$$

where N_j = number density of emitting state j, $g_i = 2J + 1$ = degeneracy of state J, $\Delta E_{i,j}$ = energy difference between state emitting states i and j, and T = electronic temperature.

A single electronic temperature does not adequately represent all the observed spectra, indicating that the plume is dominated by non-equilibrium kinetics. However, the temperature obtained from comparing the neutral yttrium $^2D^o_{5/2} \rightarrow {}^2D_{5/2}$ and $^4F^o_{7/2} \rightarrow {}^4F_{7/2}$ emission lines as shown in Fig. 5, indicates only a weak dependence on deposition laser energy. The distribution among the fine structure split $^3D^o_j$ states shown in Fig. 3 is best represented by a temperature of $T(Ba^3D) = 1100 \pm 400$ K. The error bound is considerably larger since there is a significantly smaller energy difference between these states. Regardless, the distribution among electronically excited states cannot be described by a single temperature, and the plume remains collisionally dynamic even at high pressures and low laser energies.

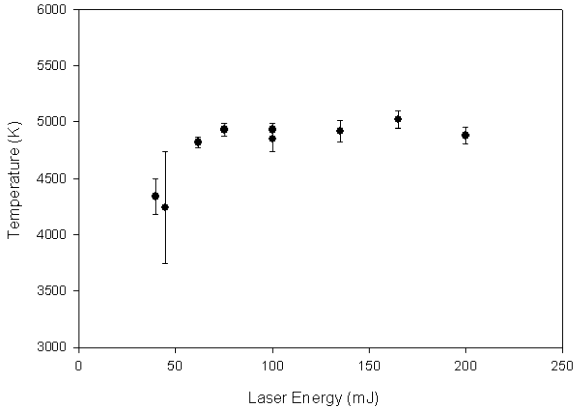

Fig. 5. Electronic temperature for the PLD plume with a 5 Torr oxygen background pressure as derived from the relative intensity of the neutral yttrium $^2D^o_{5/2} \rightarrow {}^2D_{5/2}$ and $^4F^o_{7/2} \rightarrow {}^4F_{7/2}$ emission lines.

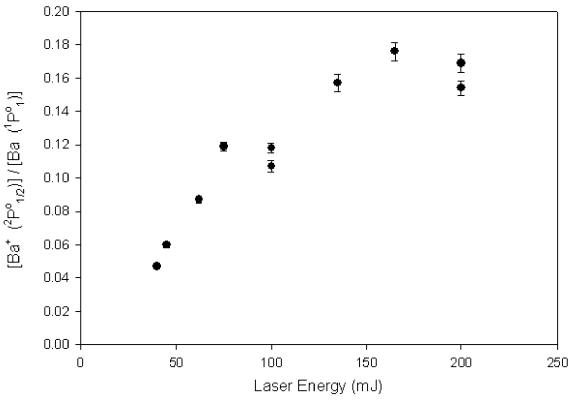

Fig. 6. Relative concentration of Ba II $^2P^o_{1,2}$ and Ba I $^1P^o_1$ as a function of ablation laser energy per pulse.

Similarly the ionic content of the plume is shown in Fig. 6. The ionization potential for barium is 5.19 eV. Clearly, the plume retains considerable excitation even when the total plume emission is low and nanoparticles are formed.

4. Conclusions

These results demonstrate that it is feasible to synthesize nanoparticles from YBCO by PLD. The nanoparticles were synthesized by the same system that was used to deposit YBCO thin films. Other than the substrate temperature which may not be important, the primary change was the background pressure of oxygen and the laser energy. YBCO nanoparticles are only formed under low laser fluence and high oxygen pressure conditions where the visible plume is largely quenched. It may be possible, although not demonstrated here, to produce YBCO thin films with nanoparticle inclusions for enhanced flux pinning. Although there are several important issues that need to be addressed with an actual demonstration of the proposed pinning mechanism, the creation of the nanoparticles themselves has been demonstrated.

Acknowledgements

This work was supported by the National Research Council (NRC) Summer Faculty Fellowship Program, AFOSR, and AFRL. The TEM measurements were done by Dr. Kevin Leedy of AFRL/SN and the AFM and STM measurements were done by Mr. Larry Grazulis of AFRL/ML.

References

[1] D.T. Verbelyi, D.K. Christen, R. Feenstra, C. Cantoni, A. Goyal, D.F. Lee, M. Paranthaman, P.N. Arendt, R.F. DePaula, J.R. Groves, C. Prouteau, Appl. Phys. Lett. 76 (2000) 1755.
[2] D.K. Finnemore, K.E. Gray, M.P. Maley, D.O. Welch, D.K. Christen, D.M. Kroeger, Physica C 320 (1999) 1.
[3] P.N. Barnes, Electric Ships Conference, Washington, DC, 2001.
[4] I. Matsubara, M. Paranthaman, T.G. Chirayil, E.Y. Sun, P.M. Martin, D.M. Kroeger, D.T. Verebelyi, D.K. Christien, Jpn. J. Appl. Phys. 38 (1999) L727.
[5] M.W. Rupich, Q. Li, S. Annavarapu, C. Thieme, W. Zhang, V. Prunier, M. Paranthaman, A. Goyal, D.F. Lee, E.D. Specht, F.A. List, IEEE Trans. Appl. Supercond. 11 (2001) 2927.
[6] V. Selvamanickam, G.B. Galinski, G. Carota, J. DeFrank, C. Trautwein, P. Haldar, U. Balachandran, M. Chudzik, J.Y. Coulter, P.N. Arendt, J.R. Groves, R.F. DePaula, B.E. Newnam, D.E. Peterson, Physica C 333 (2000) 155.
[7] S.S. Shoup, S. Shanmugham, D. Cousins, A.T. Hunt, M. Paranthaman, A. Goyal, P. Martin, D.M. Kroeger, IEEE Trans. Appl. Supercond. 9 (1999) 2426.
[8] S.R. Foltyn, E.J. Peterson, J.Y. Coulter, P.N. Arendt, Q.X. Jia, P.C. Dowden, M.P. Maley, X.D. Wu, D.E. Peterson, J. Mater. Res. 12 (1997) 2941.
[9] C. Varanasi, R. Biggers, I. Maartense, T.L. Peterson, J. Solomon, E.K. Moser, D. Dempsey, J. Busbee, D. Liptak, G. Kozlowski, R. Nekkanti, C.E. Oberly, Physica C 297 (1998) 262.
[10] S. Foltyn, P. Dowden, P. Arendt, Y. Coulter, US Department of Energy Superconductivity Program for Electric Systems Annual Peer Review, Washington, DC, 2000.
[11] J.R. Thompson, D. Paul, Z.L. Wang, D.M. Kroeger, D.M. Christen, Appl. Phys. Lett. 67 (1995) 1007.
[12] Y. Feng, A.K. Pradhan, S. Shibata, T. Machi, N. Koshizuka, IEEE Trans. Appl. Supercond. 11 (2001) 3639.
[13] G. Ghigo, A. Chiodoni, R. Gerbaldo, L. Gozzelino, B. Minetti, E. Mezzetti, C. Camerlingo, C. Giannini, IEEE Trans. Appl. Supercond. 11 (2001) 3647.
[14] P. Yang, C.M. Lieber, J. Mater. Res. 12 (1997) 2981.
[15] A. Berenov, A. Crossley, J. Wells, Y. Li, A.D. Caplin, J.L. MacManus-Driscoll, Appl. Supercond. 2 (2000) 787.
[16] L.T. Canham, Appl. Phys. Lett. 57 (1990) 1046.
[17] H. Takagi, H. Ogawa, Y. Yamazaki, A. Ishizaki, T. Nakagiri, Appl. Phys. Lett. 56 (1990) 2379.
[18] S. Furukawa, T. Miyasato, Jpn. J. Appl. Phys. 27 (1988) L2207.
[19] T.A. Burr, A.A. Seraphin, E. Werwa, K.D. Kolenbrander, Phys. Rev. B 56 (1997) 4818.
[20] D.B. Geohegan, A.A. Puretzky, G. Duscher, S.J. Pennycook, Appl. Phys. Lett. 72 (1998) 2987.
[21] K. Hata, M. Fujita, S. Yoshida, S. Yasuda, T. Makimura, K. Murakami, H. Shigekawa, W. Mizutani, H. Tokumoto, Appl. Phys. Lett. 79 (2001) 692.
[22] D.H. Lowndes, C.M. Rouleau, T. Thundat, G. Duscher, E.A. Kenik, S.J. Pennycook, Appl. Surf. Sci. 129 (1998) 355.
[23] D.H. Lowndes, C.M. Rouleau, T. Thundat, G. Duscher, E.A. Kenik, S.J. Pennycook, J. Mater. Res. 14 (1999) 359.
[24] T. Makimura, Y. Kunii, N. Ono, K. Murakami, Appl. Surf. Sci. 129 (1998) 388.
[25] T. Makino, N. Suzuki, Y. Yamada, T. Yoshida, T. Seto, N. Aya, Appl. Phys. A 69 (1999) S243.
[26] A.A. Seraphin, E. Werwa, K.D. Kolenbrander, J. Mater. Res. 12 (1997) 3386.
[27] Y.H. Tang, X.H. Sun, F.C.K. Au, L.S. Liao, H.Y. Peng, C.S. Lee, S.T. Lee, T.K. Sham, Appl. Phys. Lett. 79 (2001) 1673.
[28] Y. Zhu, H. Wang, P.P. Ong, J. Phys. D 33 (2000) 2687.
[29] Y. Zhu, P.P. Ong, Surf. Rev. Lett. 8 (2001) 559.
[30] P. Pradel, P. Monchicourt, J.J. Laucagne, M. PerDix, G. Watel, Chem. Phys. Lett. 158 (1989) 412.
[31] M. Yudasaka, Y. Ichihashi, T. Komatsu, S. Lijima, Chem. Phys. Lett. 299 (1999) 91.
[32] R. Payling, P. Larkins, Optical emission lines of the elements, John Wiley and Sons, West Sussex, England, 2000.
[33] A.H. El-Astal, S. Ikram, T. Morrow, W.G. Graham, D.G. Walmsley, J. Appl. Phys. 77 (1995) 6572.